Biosensors and Bioelectronics 85 (2016) 935–942

Contents lists available at ScienceDirect

Biosensors and Bioelectronics

journal homepage: www.elsevier.com/locate/bios

ELP-OPH/BSA/TiO_2 nanofibers/c-MWCNTs based biosensor for sensitive and selective determination of *p*-nitrophenyl substituted organophosphate pesticides in aqueous system

Jing Bao [a,b], Changjun Hou [a,*], Qiuchen Dong [b], Xiaoyu Ma [b], Jun Chen [b], Danqun Huo [a], Mei Yang [a], Khaled Hussein Abd El Galil [c], Wilfred Chen [d], Yu Lei [b,e,**]

[a] Key Laboratory of Biorheological Science and Technology (Chongqing University), Ministry of Education, Bioengineering College, Chongqing University, Chongqing 400030, China
[b] Department of Biomedical Engineering, University of Connecticut, Storrs, CT 06269, USA
[c] Department of Microbiology, Faculty of Pharmacy, Mansoura University, Egypt
[d] Department of Chemical and Biomolecular Engineering, University of Delaware, Newark, DE 19716, USA
[e] Department of Chemical and Biomolecular Engineering, University of Connecticut, Storrs, CT 06269, USA

ARTICLE INFO

Article history:
Received 30 January 2016
Received in revised form
13 May 2016
Accepted 30 May 2016
Available online 31 May 2016

Keywords:
ELP-OPH
Titanium dioxide nanofibers
Multi-walled carbon nanotubes
Methyl parathion
Parathion

ABSTRACT

A novel biosensor for rapid, sensitive and selective monitoring of *p*-nitrophenyl substituted organophosphate pesticides (OPs) in aqueous system was developed using a functional nanocomposite which consists of elastin-like-polypeptide-organophosphate hydrolase (ELP-OPH), bovine serum albumin (BSA), titanium dioxide nanofibers (TiO_2NFs) and carboxylic acid functionalized multi-walled carbon nanotubes (c-MWCNTs). ELP-OPH was simply purified from genetically engineered *Escherichia coli* based on the unique phase transition of ELP and thus served as biocatalyst for OPs, while BSA was used to stabilize OPH activity in the nanocomposite. TiO_2NFs was employed to enrich organophosphates in the nanocomposite due to its strong affinity with phosphoric group in OPs, while c-MWCNTs was used to enhance the electron transfer in the amperometric detection as well as for covalent immobilization of ELP-OPH. ELP-OPH/BSA/TiO_2NFs/c-MWCNTs nanocomposite were systematically characterized using field emission scanning electron microscopy (SEM), Raman spectra, Fourier Transform infrared spectroscopy (FTIR) and X-ray Diffraction (XRD). Under the optimized operating conditions, the ELP-OPH/BSA/TiO_2NFs/c-MWCNTs based biosensor for OPs shows a wide linear range, a fast response (less than 5 s) and limits of detection (S/N=3) as low as 12 nM and 10 nM for methyl parathion and parathion, respectively. Such excellent sensing performance can be attributed to the synergistic effects of the individual components in the nanocomposite. Its further application for selectively monitoring OPs compounds spiked in lake water samples was also demonstrated with good accuracy. These features indicate that the developed nanocomposite offers an excellent biosensing platform for rapid, sensitive and selective detection of organophosphates compounds.

1. Introduction

Highly neurotoxic organophosphates (OPs) have been widely used as pesticides and insecticides and also have the potential to be used as chemical warfare agents by terrorists, thus imposing significant strains on public health, environmental/food safety and homeland security (Giordano and Collins, 2007; Kumar et al., 2015). As OPs especially *p*-nitrophenyl OPs (e.g., methyl parathion, parathion and paraxon, etc.) are extremely toxic and it is still a big challenge to remove the residues of OP compounds from contaminated water, many countries have imposed strict restrictive regulations on the maximum concentration of OP residues in water system (Li et al., 2014). Up to date, a wide spectrum of conventional analytical methods have been developed for the determination of OPs in water samples, including gas and liquid chromatography (Oliveira et al., 2008; Walorczyk, 2007; White and Harmon, 2005), chemoluminescence (Hu et al., 2010), high-performance liquid chromatography (Perez-Ruiz et al., 2005), capillary electrophoresis (Chen and Fung, 2010), and mass

* Corresponding author.
** Corresponding author at: Department of Chemical and Biomolecular Engineering, University of Connecticut, Storrs, CT 06269, USA.
E-mail addresses: houcj@cqu.edu.cn (C. Hou), ylei@engr.uconn.edu (Y. Lei).

http://dx.doi.org/10.1016/j.bios.2016.05.094
0956-5663/

spectrometry (Fidder et al., 2002). These conventional analytical technologies offer highly sensitive and accurate assays of OPs, but also suffer from many disadvantages such as time-consuming procedures, the use of bulk and expensive instruments and requirement of skilled personnel. Therefore, they are not suitable for in-field application. Consequently, there is an urgent need to develop a simple, sensitive, low-cost and rapid method for OPs detection.

In the past decade, enzyme-based electrochemical biosensors for OPs have been becoming a promising method in this regard. Unlike acetylcholinesterase (AChE) based single-use OP biosensors which rely on the non-selective and irreversible inhibition of the enzyme activity, organophosphorus hydrolase (OPH) based OP biosensors are more attractive as OPH can selectively hydrolyze a wide range of OPs, thus endowing the reusability of OPH-based biosensors in OPs determination (Wang et al., 1999; Chough et al., 2002; Lei et al., 2005a, 2005b; Liu et al., 2014; A. Mulchandani et al., 2001a; P. Mulchandani et al., 2001b; Mulchandani et al., 2006). Specifically, *p*-nitrophenyl substituent OPs can be catalyzed by OPH to generate electroactive *p*-nitrophenol (PNP), and the oxidation current of PNP can be correlated to the OP concentration in amperometric detection, which offers a convenient biosensing platform (Tang et al., 2014; Stoytcheva et al., 2014). However, to purify OPH is tedious and time-consuming, which could limit its wide applications. Therefore, in this study, elastin-like polypeptide fused with organophosphorus hydrolase (ELP-OPH) was constructed to allow a very simple and rapid method for ELP-OPH purification based on the temperature-triggered phase transition of ELP (Shimazu et al., 2003). Moreover, the ELP domain could also improve the stability of the fusion enzyme. However, OPH or ELP-OPH is intrinsically no-conducting, which is not favorable for electrochemical sensing application. Therefore, in recent years, nanomaterials have been exploited to enhance electron transport and promote oxidation of electroactive compounds on the sensing electrodes, which could result in OPs biosensors with high performance. For example, the discovery of carbon nanotubes (CNTs) in 1991 has brought increasing attentions in academic and research area owing to its unique chemical and physical properties (IIJIMA, 1991). Particularly, carbon nanotube (CNT) has been reported as an excellent sorbent and good electrocatalytic nanomaterial for aromatic OP detection due to its π-conjugative interaction upon the benzene ring and high conductivity (Zhang et al., 2003; Yan et al., 2005; Zhou et al., 2007). Carboxylic acid functionalized multi-walled carbon nanotubes (c-MWCNTs) are also attractive in biosensor applications due to their advanced mechanical property and excellent electrical conductivity. Moreover, their carboxylic groups can provide a large number of covalent or non-covalent binding sites for enzyme immobilization, thus significantly improving analytical performance of sensors (Pedrosa et al., 2010). Some transition metal oxides such as zirconium dioxide (ZrO_2) and titanium oxide (TiO_2) have also been widely used for selectively enriching free OP compounds due to their strong affinity with the phosphoric group in OPs as well as their low price, long-term chemical stability and good biocompatibility (Du et al., 2011; Bavykin et al., 2006a, 2006b; Huang et al., 2010; Kweon and Hakansson, 2006; Yang et al., 2012). All these studies suggest that high performance biosensors could be developed by taking use of the synergistic effects of individual components in nanocomposites.

In this work, a novel nanocomposite-based biosensor, consisting of ELP-OPH, bovine serum albumin (BSA), TiO_2 nanofibers (TiO_2NFs) and c-MWCNTs, was developed for rapid, sensitive and selective determination of organophosphate (OP) pesticides. Unique thermal-triggered phase-transition of ELP was employed to simply purify ELP-OPH (serving as biocatalyst for OPs) from genetically engineered *Escherichia coli* through two cycles of centrifuge, while BSA, TiO_2NFs and c-MWCNTs in the nanocomposite will be used to stabilize OPH activity, to enrich organophosphates in the nanocomposite, and to covalently immobilize ELP-OPH/BSA and enhance the electron transfer in the amperometric detection, respectively. The micromorphology and structure of the as-prepared ELP-OPH/BSA/TiO_2NFs/c-MWCNTs nanocomposite were systematically characterized using scanning electron microscopy (SEM), Raman, Fourier transform infrared spectroscopy (FTIR) and X-ray powder diffraction (XRD). The as-developed OP biosensor was optimized in terms of material loading and the applied potential. Under the optimal conditions, ultra-sensitive amperometric detection of methyl parathion and parathion in both buffer and spiked lake water samples was realized. These features indicate that the developed nanocomposite offers an excellent biosensing platform for rapid, sensitive and selective detection of organophosphates compounds, which could have the potential to play an important role in securing public health, environmental/food safety and homeland security.

2. Experimental part

2.1. Reagents and materials

Genetically engineered *Escherichia coli* with ELP-OPH expression was constructed according to a procedure reported elsewhere (Shimazu et al., 2003). Titanium isopropoxide ($Ti(OiPr)_4$, 97%), polyvinylpyrrolidone (PVP, MW=1300,000 g/mol), c-MWCNTs, Nafion 117 solution, and N, N-dimethylformamide (DMF, anhydrous, 99.8%) were purchased from Sigma-Aldrich. Methyl parathion and parathion were purchased from SUPELCO Analytical (USA) and used without further purification. 1-ethyl-3-(3-dimethylaminopropyl) carbodiimide (EDC) and N-hydroxysuccinimide (NHS) were bought from Thermo Scientific (USA), while bovine serum albumin (BSA) was purchased from Bio-Rad (USA). Lake water samples were collected from Hollow Lake (Mansfield, Connecticut, USA). All aqueous solutions were freshly prepared with deionized (DI) water (18 MΩ cm) generated by a Barnstead DI water system.

2.2. Electrode preparation and modification

2.2.1. Preparation of ELP–OPH and TiO_2 NFs

The ELP-OPH was purified from cell culture according to a phase-transition method reported elsewhere (Shimazu et al., 2003) and the final stock concentration was determined to be 2 mg/mL with OPH activity (for methyl parathion) of 3785 IU/mg. Titanium dioxide nanofibers were prepared using electrospinning followed by calcination, according to the procedure reported in our previous publication (Ding et al., 2011).

2.2.2. Preparation of the ELP-OPH/BSA/TiO_2NFs/c-MWCNTs nanocomposite modified electrodes

Prior to the surface modification, the bare glassy carbon electrode (GCE, dia. 3 mm) was polished with 0.3 μm and 0.05 μm alumina slurries successively, and then sonicated with acetone, ethanol and DI water in sequence to remove any alumina residue on the electrode surface. 2 mg TiO_2NFs and 0.5 mg c-MWCNTs were homogenously dispersed in 1 mL DMF through 30-min sonication, respectively, and then 6 μL of TiO_2NFs and c-MWCNTs mixture were prepared with an appropriate volume ratio of TiO_2NFs suspension and c-MWCNTs suspension and directly drop-cast onto the surface of GCE. Next, 10 μL Nafion (NF) solution (0.05 wt%) was loaded on the modified GCE to dry at room temperature, thus forming highly porous Nafion membrane to entrap TiO_2NFs/c-MWCNTs on GCE. Subsequently, the as-prepared

TiO_2NFs/c-MWCNTs electrodes were immersed into freshly prepared EDC (2 mg/mL)/NHS (10 mg/mL) solution to active the carboxylic groups on c-MWCNTs surface for 20 min. After drying in air, 8 μL of ELP-OPH/BSA (1/1, v/v) solution was coated on the as-prepared TiO_2NFs/c-MWCNTs electrodes surface for 2 h cross-linking to immobilize the ELP-OPH/BSA on the activated c-MWCNTs, followed by extensively rinsed with 0.05 M pH 7.4 PBS buffer. The as-prepared electrode is denoted as ELP-OPH/BSA/TiO_2NFs/c-MWCNTs/GCE. In addition, control electrodes including bare GCE, c-MWCNTs/GCE and ELP-OPH/BSA/c-MWCNTs/GCE are also prepared to elucidate the role of individual component in OP biosensing.

2.3. Characterization and electrochemical measurements

The morphology of the as-prepared samples was obtained using a JEOL 6335F field emission scanning electron microscopy (FESEM) at an acceleration voltage of 10 kV. Raman spectra were collected using a Renishaw 2000 Ramanscope Micro-Raman coupled with a 514 nm argon-ion laser (50 mW). FTIR spectra and XRD patterns of the samples were performed on Nicolet Magna-IR 560 spectrophotometer and Oxford diffraction XcaliburTM PX Ultra with ONYX detector, respectively. The absorption spectra to study the interaction between TiO_2NFs and methyl parathion were obtained using a Cary 50 UV–vis spectrophotometer (Agilent Technologies). Cyclic voltammetric (CV), amperometry (i–t), differential pulse voltammetry (DPV) and electrochemical impedance spectroscopy (EIS) measurements were carried out using a CHI 660D electrochemical workstation (CH Instrument, USA) with the modified GCE electrode, Ag/AgCl (3 M KCl) electrode and Pt wire as the working, the reference and auxiliary electrodes, respectively. All the measurements were triplicated and recorded at room temperature.

3. Results and discussion

3.1. Purification and characterization of ELP-OPH

The elastin-like-polypeptide (ELP) as the thermal-responsive purification tag offers simple purification and reversible immobilization of ELP-OPH (Shimazu et al., 2003). Cells (genetically engineered *Escherichia coli* with expressed ELP-OPH) were grown in LB broth at 37 °C with shaking and harvested after 2 days of incubation and the cell lysate was harvested through ultra-sonication and centrifugation at 4 °C. Then 2 M NaCl was added to the cell lysate and the mixture was incubated at 37 °C. The resulting pellet containing ELP-OPH was recovered after centrifugation. After solubilization at 4 °C, the supernatant was subject to an additional round of inverse temperature cycling resulting in highly purified ELP-OPH. Purified ELP-OPH fusion protein (20 L) was then analyzed on 8% SDS-PAGE gel. As shown in Fig. S1, after two-cycle purification, relatively pure ELP-OPH with a molecular weight of ~60 kDa was obtained. The size is slightly smaller than the expected value because of the low percentage gel used. The final ELP-OPH concentration was determined to be 2 mg/mL through protein analysis by UV – vis spectrophotometer and the OPH activity expressed as μmol of methyl parathion hydrolyzed to generate *p*-nitrophenol per min (U) per mg through OPH activity assay and the activity value was 3785 IU/mg (Shimazu et al., 2001).

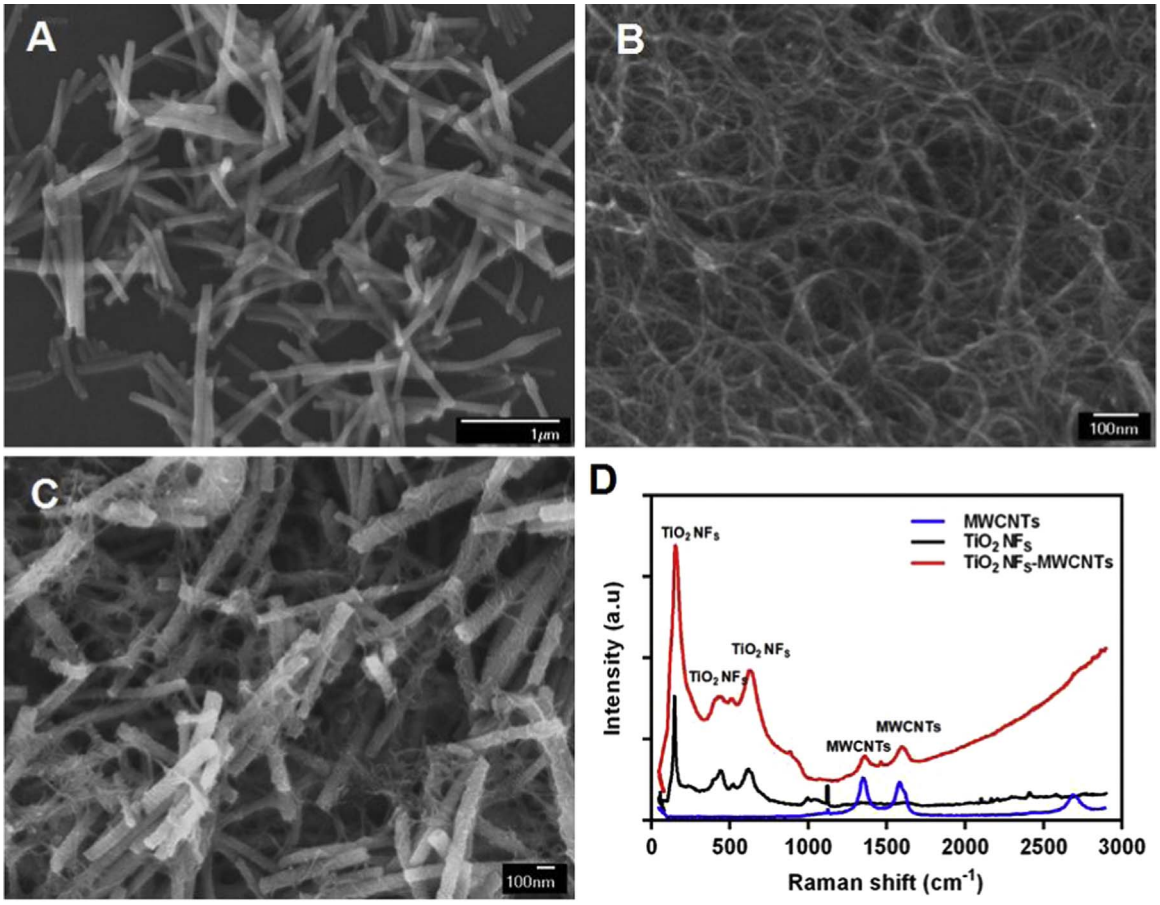

Fig. 1. SEM images of TiO_2NFs **(A),** c-MWCNTs **(B),** and TiO_2 NFs/c-MWCNTs hybrid composite **(C)**, respectively. (D) Raman spectra of TiO_2NFs/c-MWCNTs hybrid nanocomposite.

3.2. Characterization of the as-prepared TiO_2NFs/c-MWCNTs hybrid composite

The morphology of the as-prepared TiO_2NFs/ c-MWCNTs composites was first investigated by SEM. As shown in Fig. 1A, TiO_2NFs exhibit uniform rod structure with an average diameter of 80 ± 20 nm, while c-MWCNTs (dia.: 15 ± 5 nm) entangle with each other to form mesh structure (Fig. 1B). FTIR study (Fig. S2A) of c-MWCNTs shows the peaks around 1658 (C=O) and 1100 (C–O) cm^{-1}, distinctly corresponding to the stretching mode of the carboxylic acid group (–COOH) of the c-MWCNTs (Park et al., 2009). It is worth noting that the TiO_2NFs/c-MWCNTs hybrid composite form a highly-intensive, intertangled network structure (Fig. 1C), in which the entangled c-MWCNTs could provide good electron transfer as well as a number of –COOH groups for covalent immobilization of OPH, and TiO_2NFs could offer high binding affinity with OPs, thus enriching local OPs concentration to OPH in the final OP detection.

Raman spectra were also collected for the nanocomposites. As shown in Fig. 1D, two prominent Raman bands at 1360 cm^{-1} and 1604 cm^{-1} are assigned to the Disorder mode and Tangential mode of c-MWCNTs (Atchison et al., 2015; Hariharasubramanian et al., 2014), respectively, while the Raman bands at 145 cm^{-1}, 451 cm^{-1} and 637 cm^{-1} are ascribed to three active E_g modes of the TiO_2 nanofibers (Nasr et al., 2015). FTIR study also indicates the presence of –COOH group (Fig. S2A). The crystalline structures of TiO_2NFs/c-MWCNTs nanocomposite were further revealed by XRD analysis (Fig. S2B). The diffraction peaks located at 2θ values of 26.05°, 41.04°, 55.03°and 62.8°, correspond to (101), (200), (211) and (204) crystal planes of the TiO_2 nanofibers (Li and Xia, 2003), respectively, while the diffraction peaks at 2θ value of 25.5° and 42.75° are assigned to (002) and (001) planes in c-MWCNTs (Hariharasubramanian et al., 2014). All these results suggest the successful preparation of TiO_2NFs/c-MWCNTs nanocomposites, which could provide not only a large number of carboxylic acid sites for enzyme immobilization, but also highly meshed structure with entangled c-MWCNTs as the electron conduction channels, which is favorable for the electrochemical biosensor application.

3.3. Electrochemical behavior of the as-prepared biosensors in the absence and presence of methyl parathion

In order to study the feasibility of using ELP-OPH for OP detection, ELP-OPH was immobilized on GCE using Nafion and then cyclic voltammetry (CV) was first employed to investigate the electrochemical behavior of the as-prepared electrode in 0.05 M pH 7.4 PBS buffer solution containing 0 mM, 0.2 mM, and 0.5 mM methyl parathion, respectively. Fig. 2A displays a concentration-dependent oxidation peak at ca. +0.93 V in the presence of 0.2 mM and 0.5 mM methyl parathion, which can be attributed to the electrochemical oxidation of *p*-nitrophenol (PNP) (Scheme 1), liberated from OPH-catalyzed hydrolysis of methyl parathion. (Karami et al., 2014; Stoytcheva et al., 2014). However, the oxidation peak current is weak in magnitude, and thus nanocomposite (ELP-OPH/BSA/TiO_2NFs/c-MWCNTs) was developed to enhance the signal. In order to understand the role of individual component in nanocomposites in enhancing the electrochemical signal, CVs of four electrodes with different material composition in 0.05 M pH 7.4 PBS buffer solution containing 0.5 mM methyl parathion were collected and shown in Fig. 2B. Compared to the signal obtained on the bare GCE (Fig. 2B, trace a), the incorporation of c-MWCNTs (c-MWCNTs/GCE) enhanced the background current (Fig. 2B, trace b), but no prominent oxidation peak was observed. Upon the immobilization of ELP-OPH/BSA on c-MWCNTs, the oxidation peak current at the ELP-OPH/BSA/c-MWCNTs/GCE was significantly enhanced (Fig. 2B, trace c). It is mainly attributed to

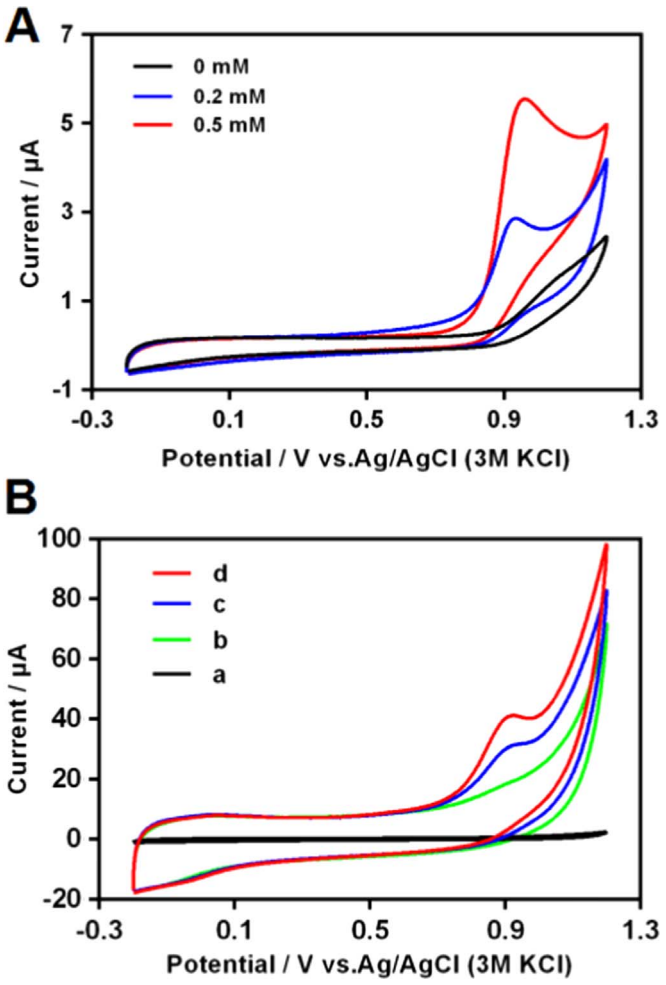

Fig. 2. (A) CVs of the ELP-OPH/BSA/GCE in 0.05 M pH 7.4 PBS buffer containing 0 mM, 0.2 mM, and 0.5 mM methyl parathion, respectively. **(B)** CVs of the different electrodes in 0.05 M pH 7.4 PBS buffer containing 0.5 mM methyl parathion: a) GCE; b) c-MWCNTs/GCE; c) ELP-OPH/BSA/c-MWCNTs/GCE; and d) ELP-OPH/BSA/TiO_2NFs/ c-MWCNTs/GCE. The scan rate is 0.10 V/s.

the catalytic activity of OPH for methyl parathion as well as the enhanced conductivity resulted from c-MWCNTs (Du et al., 2008; Pedrosa et al., 2010). The highest oxidation peak was obtained at the ELP-OPH/BSA/TiO_2NFs/c-MWCNTs/GCE (Fig. 2B, trace d). The incorporation of TiO_2NFs into nanocomposite results in the oxidation peak sharper, which was also supported by Fig. 3B using ELP-OPH/BSA/TiO_2NFs/c-MWCNTs/GCE in the study. Such sharper peak favors DPV detection of OPs. One can see that methyl parathion as low as 200 nM can be easily detected using DPV on the ELP-OPH/BSA/TiO_2NFs/c-MWCNTs/GCE. In order to further elucidate the role of TiO_2NFs, UV–vis spectrometry was used to evaluate the adsorption of methyl parathion by TiO_2NFs. PNP, a hydrolysis product of methyl parathion by OPH, displays yellowish color with a characteristic UV–vis absorption peak at 406 nm. As shown in Fig. 3A, the freshly prepared 1 mM methyl parathion solution upon the addition of 50 µL ELP-OPH (Inset of Fig. 3A, bottle b) displayed a light yellow color with a prominent absorption peak at 405 nm (Fig. 3A, curve b) due to the generation of PNP. However, when 1 mM methyl parathion solution was first treated with TiO_2NFs for adsorption and removal, the addition of OPH did not generate obvious yellow color (Inset of Fig. 3A, bottle a), corroborated by the much weaker absorption peak at 406 nm (Fig. 3A, curve a). This study indicates that significant amount of methyl parathion was adsorbed and removed by TiO_2NFs. Such excellent adsorption ability of TiO_2NFs can be attributed to its strong affinity

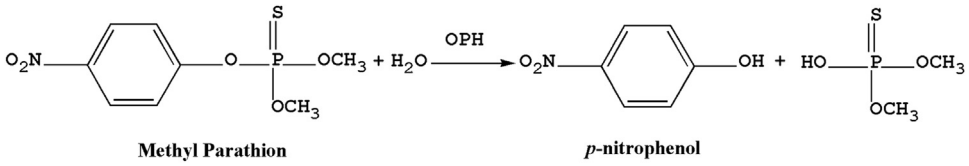

Scheme 1. Reaction Scheme for the OPH-catalyzed hydrolysis of methyl parathion.

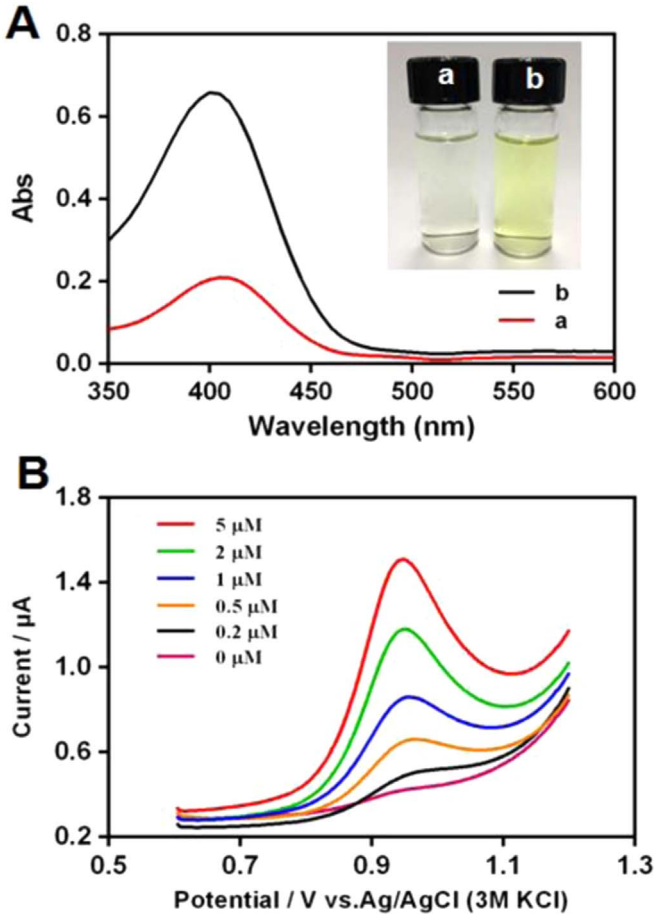

Fig. 3. (A) UV–vis absorbance spectra of different samples: (a) 1 mM methyl parathion was first treated with 1 mg TiO_2NFs for 15 min and then TiO_2NFs were removed by centrifuge, followed by the addition of 50 μL ELP-OPH; and (b) 1 mM methyl parathion with the addition of 50 μL ELP-OPH. The inset shows the optical image of samples in (a) and (b), respectively. **(B)** DPVs on the ELP-OPH/BSA/TiO_2NFs/c-MWCNTs/GCE in 0.05 M pH 7.4 PBS containing different concentration of methyl parathion (from bottom to top, 0 μM, 0.2 μM, 0.5 μM, 1 μM, 2 μM, and 5 μM, respectively).

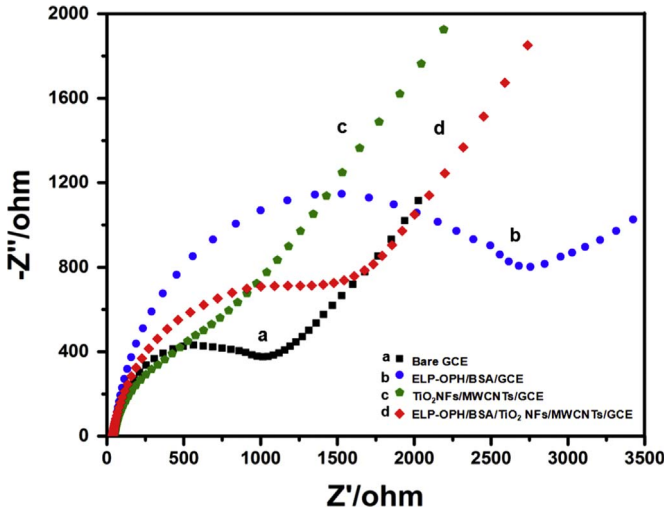

Fig. 4. Electrochemical impedance spectra (EIS) of (a) bare GCE, (b) ELP-OPH/BSA/GCE, (c) TiO_2NFs/c-MWCNTs/GCE, and (d) ELP-OPH/BSA/TiO_2 NFs/c-MWCNTs/GCE recorded in 0.05 M pH 7.4 PBS containing 10 mM $K_3Fe(CN)_6$ and $K_4Fe(CN)_6$.

with the phosphoric group in methyl parathion (Yang et al., 2012; Kweon and Hakansson, 2006).

Based on aforementioned discussion, such good performance of the nanocomposite can be attributed to the synergistic effect of good adsorption of methyl parathion on TiO_2NFs, enhanced electron transfer by c-MWCNTs and the proximity of OPH enzyme to c-MWCNTs and enriched methyl parathion in the nanocomposites, favoring the generation of PNP and its subsequent electrochemical oxidation and electron transfer (Wang et al., 2011; Bavykin et al., 2006a, 2006b).

3.4. Electrochemical impedance spectroscopy (EIS)

Electrochemical impedance spectroscopy (EIS) is a useful technique to study the electronic transfer properties and the impedance changes of surface modified electrodes (Dervisevic et al., 2015; Du et al., 2010). To further elucidate the role of c-MWCNTs in the enhancement of electron transfer, EIS was carried out for four representative electrodes. Fig. 4 illustrates the Nyquist plots of bare GCE, ELP-OPH/BSA/GCE, TiO_2NFs/c-MWCNTs/GCE and ELP-OPH/BSA/TiO_2NFs/c-MWCNTs/GCE using 10 mM $Fe(CN)_6^{3-/4-}$ as the redox probe in the frequency range from 10^{-1} to 10^5 Hz. The diameter of semicircle at higher frequencies corresponds to the electron transfer limited process and can be used as the indicator of the electron transfer resistance (R_{ct}). As shown in Nyquist Impedance Circular Fitting Plots (Supplementary material, Fig. S3), the coating of ELP-OPH/BSA on GCE increases GCE's R_{ct} from 1120 Ω (Fig. S3A) to 2912 Ω (Fig. S3B), which can be attributed to the poor conductivity of protein/enzyme. However, compared to bare GCE, the R_{ct} of TiO_2NFs/c-MWCNTs/GCE is ~883 Ω (Fig. S3C), suggesting that TiO_2NFs/ c-MWCNTs composite greatly enhances the electron transfer efficiency due to the excellent conductivity of c-MWCNTs. After the covalent immobilization of ELP-OPH/BSA on the TiO_2NFs/c-MWCNTs/GCE, the R_{ct} increases to 2008 Ω (Fig. S3D). Such increase of R_{ct} can be attributed to the successfully covalent immobilization of ELP-OPH/BSA on carboxylic acid functionalized c-MWCNTs, which could partially block the interfacial electron transfer (Wang et al., 2011).

3.5. Optimization of the ELP-OPH/BSA/TiO_2NFs/c-MWCNTs biosensor

In order to further optimize the ELP-OPH/BSA/TiO_2NFs/c-MWCNTs based biosensor, the effects of the loading of ELP-OPH/BSA, the ratio of TiO_2NFs to c-MWCNTs and the applied potential on the biosensor response to OPs were systematically investigated. During the optimization of one parameter, all other parameters are maintained at their optimal conditions.

As the total amount of ELP-OPH attached onto the surface of electrode can largely affect the biosensor response, the effect of loading volume of the mixture of ELP-OPH/BSA (concentration: 1% BSA and 1 mg/mL ELP-OPH) on the GCE electrode was optimized.

1% BSA was used to stabilize OPH (A. Mulchandani et al., 1999a; P. Mulchandani et al., 1999b). As shown in Fig. S4 (Supplementary material), with the increasing of the loading volume from 4 μL to 10 μL, the oxidation current initially increases almost linearly and then gradually levels off due to the increased loading of ELP-OPH. Since the loading volume larger than 8 μL (~30 IU OPH) was not beneficial, this loading volume of ELP-OPH/BSA was used for subsequent experiments. Furthermore, 6 μL of TiO_2NFs and c-MWCNTs mixture were prepared with an appropriate volume ratio of TiO_2NFs (2 mg/mL) and *c*-MWCNTs (0.5 mg/mL) for studying its effect on the biosensor response. As shown in Fig. S5, a ratio (v/v) of TiO_2NFs to c-MWCNTs results in the highest normalized signal. To investigate the effect of the applied potential on the biosensor response, amperometric response of the as-prepared biosensor to successive addition of 0.5 μM methyl parathion was collected at an applied potential ranging from 0.84 V to 0.96 V (vs. Ag/AgCl) with 0.03 V increment. As shown in Fig. S6, the biosensor response increased sharply up to 0.93 V and then leveled off thereafter. An applied potential of 0.93 V resulted in the maximum signal, which was used in the subsequent experiments.

3.6. Amperometric detection of methyl parathion and parathion

Under the optimal operating conditions, the current-time amperometric response of the ELP-OPH/BSA/TiO_2NFs/c-MWCNTs biosensor was generated by continuous addition of OPs (methyl parathion and parathion) from 0.1 μM to 20 μM (3 times per concentration) in 0.05 M pH 7.4 PBS buffer solution. As shown in Fig. 5A, the current response of ELP-OPH/BSA/TiO_2NFs/c-MWCNTs biosensor increased rapidly within 5 s after the addition of methyl parathion (curve a) and the response was about 6-fold higher than that of ELP-OPH/BSA biosensor (curve b). The corresponding calibration curve of ELP-OPH/BSA/TiO_2NFs/c-MWCNTs biosensor was presented in Fig. 5B, which was linear up to 36.4 μM for methyl parathion with a sensitivity of 0.1519 μA/μM (linear regression equation: $I=0.1519\cdot C+0.159$, $R^2=0.9945$) and the lower limit of detection (S/N=3) of 12 nM. The same biosensor was also applied for parathion detection and the result was presented in Fig. 5C. The corresponding calibration curve (Inset of Fig. 5C) shows that the response was also linear up to 36.4 μM for parathion with a sensitivity of 0.1647 μA/μM (linear regression equation: $I=0.1647\cdot C+0.2564$, $R^2=0.981$) and the lower limit of detection (S/N=3) of 10 nM. Particularly, the LOD values of the as-developed biosensor were calculated with the corresponding calibration plots for methyl parathion (Fig. 5B inset) and parathion (Fig. 5D inset) detected from 0.1 μM to 5.4 μM, respectively. The sensitivity and the limit of detection of this biosensor for parathion are slightly better than methyl parathion which can be attributed to higher catalytic activity of OPH towards parathion (Lei et al., 2004a, 2004b, 2005a, 2005b). The sensing performance (the linear range and the limit of detection) of the as-developed OP biosensor was also compared with other OPH-based biosensors in literature (Table 1). One can see that both the linear range and the LOD obtained in present work were among the best values, indicating the excellent sensing performance, which can be attributed to several factors such as enrichment of OPs in nanocomposite (strong adsorption between OPs and TiO_2NF), enhancement of electron transfer offered by c-MWCNTs and the proximity of enzyme to c-MWCNTs. The synergistic effect of those factors favors the generation of PNP and its subsequent electrochemical

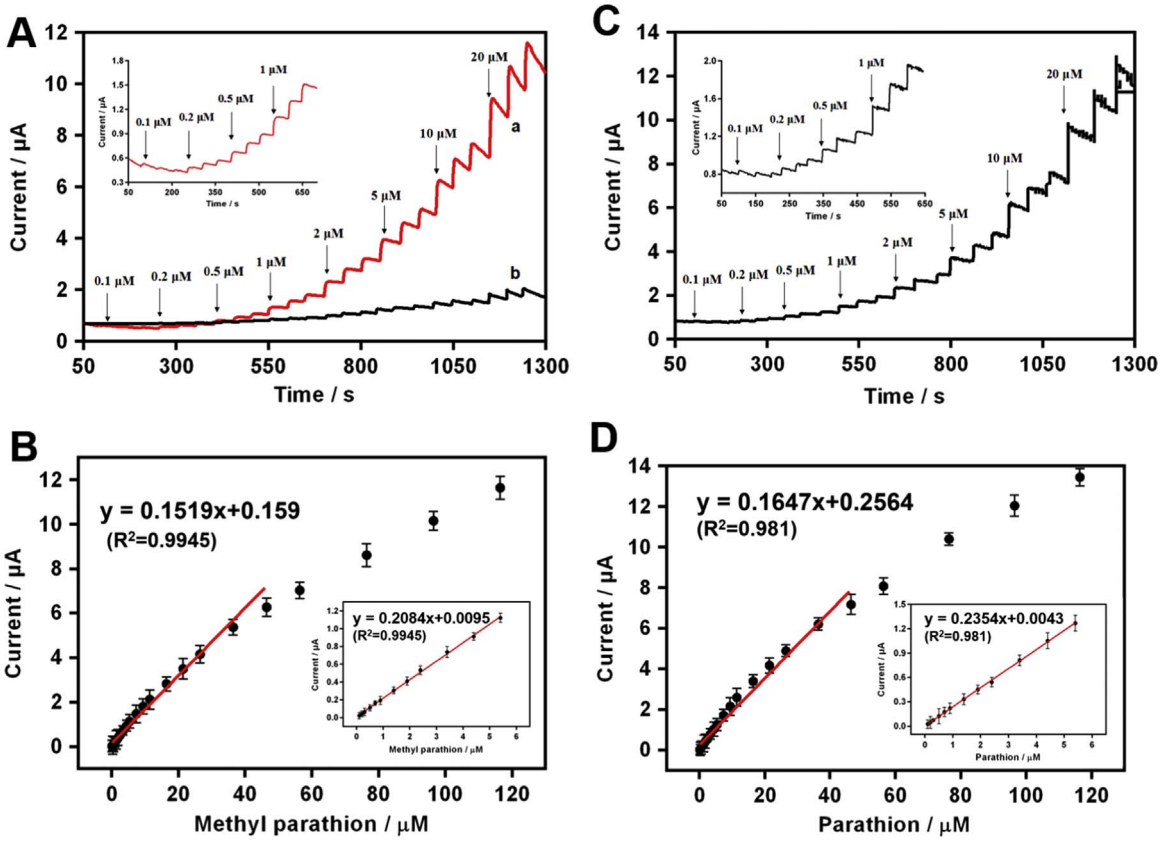

Fig. 5. Current-time response of the ELP-OPH/BSA/TiO_2NFs/c-MWCNTs/GCE (a) and ELP-OPH/BSA/GCE (b) toward continuous addition of methyl parathion **(A)** and Current-time response of the ELP-OPH/BSA/TiO_2NFs/c-MWCNTs/GCE toward continuous addition of parathion **(C)** from 0.1 μM to 20 μM in 0.05 M pH 7.4 PBS buffer solution. (Inset shows the current-time response of the ELP-OPH/BSA/TiO_2NFs/c-MWCNTs/GCE for methyl parathion and parathion detect from 0.1 μM to 1 μM). The corresponding calibration plot for methyl parathion **(B)** and parathion **(D)** detect from 0.1 μM to 20 μM. (Inset shows the corresponding calibration plots for methyl parathion and parathion detect from 0.1 μM to 5.4 μM, respectively.

Table 1.
Comparison of the ELP-OPH/BSA/TiO_2NFs/c-MWCNTs biosensor in this study with other reported OPH-based amperometric biosensors for the detection of *p*-nitrophenyl substituent OPs.

Sensing electrode	OP substrate	Linear range (μM)	LOD (nM)	Ref.
OPH/Nafion	Methyl parathion Paraoxon	Up to 5 μM	70	(A. Mulchandani et al., 1999a; P. Mulchandani et al., 1999b)
		Up to 40 μM	90	
OPH-bacteria	Methyl parathion Paraoxon	Up to 140 μM	20	(A. Mulchandani et al., 2001a; P. Mulchandani et al., 2001b)
		Up to 120 μM	20	
OPH-bacteria/OMCs	Methyl parathion Parathion	0.08–30 μM	15	(Tang et al. 2014)
		0.05–25 μM	10	
OPH/Carbon-paste	Parathion	–	15	(Chough et al. 2002)
	Paraoxon	–	20	
OPH/CNTs	Methyl parathion	2–10 μM	800	(Deo et al. 2005)
ELP-OPH/BSA/TiO_2NFs/c-MWCNTs	Methyl parathion	Up to 36.4 μM	12	Present
	Parathion	Up to 36.4 μM	10	Present

oxidation and electron transfer, thus resulting in excellent sensing performance. In addition, OPH takes OPs as substrates instead of inhibitors, and thus the reusability of the ELP-OPH/BSA/TiO_2NFs/c-MWCNTs biosensor is a significant advantage over the single-use AChE-based OP biosensors (due to the irreversible inhibition of AChE by OPs). In conjunction with simple purification of ELP-OPH based on the thermal-triggered phase transition and the reusability of the as-developed OPs biosensor based on ELP-OPH, the developed OPs biosensor provides a cost-effective and sensitive sensing platform for OPs detection.

3.7. Application of the ELP-OPH/BSA/TiO_2NFs/c-MWCNTs biosensor for spiked real water sample analysis

To further study the potential practical applications of the ELP-OPH/BSA/TiO_2NFs/ c-MWCNTs/GCE, lake water samples spiked with parathion and methyl parathion were used. The lake water sample collected from Hollow Lake, Mansfield, CT, USA was first filtered through a well-defined 0.2 μm PVDF filter to remove any large particles, and then its pH and ionic strength were adjusted to match with the buffer solution used in previous sections. The amperometric response to the injection of spiked lake water samples with different concentration of methyl parathion and parathion is presented in Fig. S7. As summarized in Table 2, the recoveries of spiked methyl parathion and parathion in real samples were observed in the range from $94.67 \pm 2.82\%$ to $106.73 \pm 2.61\%$, indicating the excellent reliability of the developed OPs biosensor. This study also corroborates that the matrix effect from real water samples did not interfere with the detection of OPs, indicating its good selectivity against naturally occurring compounds in real water samples. The long-term storage stability of the ELP-OPH/BSA/TiO_2NFs/c-MWCNTs biosensor was also an important criterion in evaluating the sensor performance; therefore, a corresponding study was carried out. When stored in 0.05 M pH 7.4 PBS buffer at 4 °C, there was no obvious decrease in the response to methyl parathion for the first 7 days. After a period of 15 days, the biosensor also retained 93% of its initial response to OPs, indicating the good stability of the as-developed biosensor and also demonstrating the ability of the ELP domain to improve the stability of OPH in conjunction with BSA. Such good recovery rates and stability of the developed OPs biosensor demonstrate that the ELP-OPH/BSA/TiO_2NFs/c-MWCNTs nanocomposite based biosensor is highly reliable and suitable for practical application.

Table 2.
Recovery studies of spiked methyl parathion and parathion in lake water samples (each result was the average of five determinations).

Pesticides	Added (μM)	Found (μM)	Recovery (%)	RSD (%)
Methyl parathion	0.50	0.473	94.67	2.82
	2.00	2.047	102.33	3.79
Parathion	0.50	0.503	100.48	4.96
	2.00	2.134	106.73	2.61

4. Conclusion

In summary, an ultrasensitive, selective and rapid ELP-OPH/BSA/TiO_2NFs/c-MWCNTs biosensor was developed for detection of *p*-nitrophenyl substituent OPs. ELP-OPH was simply purified based on thermal-triggered phase transition of ELP and then covalently immobilized to form ELP-OPH/BSA/TiO_2NFs/c-MWCNTs nanocomposite through carboxylic acid functionalized c-MWCNTs in the presence of BSA stabilizer. Under the optimal operating conditions, the ELP-OPH-BSA/TiO_2NFs/c-MWCNTs based biosensor can detect OPs with a wide linear range, a fast response (less than 5 s) and limits of detection (S/N=3) as low as 12 nM and 10 nM for methyl parathion and parathion, respectively. Such excellent sensing performance can be attributed to enrichment of OPs in nanocomposite (strong adsorption between OPs and TiO_2NF), enhancement of electron transfer by c-MWCNTs and the proximity of enzyme to c-MWCNTs and absorbed OPs in the nanocomposites, favoring the generation of electroactive PNP and its subsequent electrochemical oxidation and electron transfer. Its further application for monitoring OPs compounds spiked in lake water samples was also demonstrated with good accuracy. In conjunction with the easy purification of ELP-OPH and good stability, these features demonstrate that the developed nanocomposite based biosensor holds great promise in rapid, cost-effective, sensitive and selective detection of OPs in real water samples.

Acknowledgement

This work was financially supported by the National Natural Science Foundation of China (31171684), Chongqing's Postgraduate Research Innovation Projects (CYB14028), Key Technologies R&D Program of China (2014BAD07B02), Key Technologies R&D Program of Sichuan Province of China (2013FZ0043), Open Fund of Liquor-Making Biotech and Application Key Laboratory of Sichuan Province (NJ2014–03) and the Short-term International Academic Fund of Chongqing University 2014 Overseas Visiting Student Project Agreement. We also thank the support of sharing fund for Chongqing University's major equipment.

Appendix A. Supplementary material

Supplementary data associated with this article can be found in the online version at http://dx.doi.org/10.1016/j.bios.2016.05.094.

References

Atchison, J.S., Zeiger, M., Tolosa, A., Funke, L.M., Jaeckel, N., Presser, V., 2015. Electrospinning of ultrafine metal oxide/carbon and metal carbide/carbon nanocomposite fibers. Rsc Adv. 5 (45), 35683–35692.

Bavykin, D.V., Friedrich, J.M., Lapkin, A.A., Walsh, F.C., 2006a. Stability of aqueous suspensions of titanate nanotubes. Chem. Mater. 18 (5), 1124–1129.

Bavykin, D.V., Friedrich, J.M., Walsh, F.C., 2006b. Protonated titanates and TiO_2 nanostructured materials: synthesis, properties, and applications. Adv. Mater. 18 (21), 2807–2824.

Chen, Q., Fung, Y., 2010. Capillary electrophoresis with immobilized quantum dot fluorescence detection for rapid determination of organophosphorus pesticides in vegetables. Electrophoresis 31 (18SI), 3107–3114.

Chough, S.H., Mulchandani, A., Mulchandani, P., Chen, W., Wang, J., Rogers, K.R., 2002. Organophosphorus hydrolase-based amperometric sensor: modulation of sensitivity and substrate selectivity. Electroanalysis 14 (4), 273–276.

Deo, R.P., Wang, J., Block, I., Mulchandani, A., Joshi, K.A., Trojanowicz, M., Scholz, F., Chen, W., Lin, Y.H., 2005. Determination of organophosphate pesticides at a carbon nanotube/organophosphorus hydrolase electrochemical biosensor. Anal. Chim. Acta 530 (2), 185–189.

Dervisevic, M., Custiuc, E., Cevik, E., Senel, M., 2015. Construction of novel xanthine biosensor by using polymeric mediator/MWCNT nanocomposite layer for fish freshness detection. Food CHEM 181, 277–283.

Ding, Y., Wang, Y., Zhang, L., Zhang, H., Li, C.M., Lei, Y., 2011. Preparation of TiO_2-Pt hybrid nanofibers and their application for sensitive hydrazine detection. Nanoscale 3 (3), 1149–1157.

Du, D., Chen, A., Xie, Y., Zhang, A., Lin, Y., 2011. Nanoparticle-based immunosensor with apoferritin templated metallic phosphate label for quantification of phosphorylated acetylcholinesterase. Biosens. Bioelectron. 26 (9), 3857–3863.

Du, D., Chen, W., Zhang, W., Liu, D., Li, H., Lin, Y., 2010. Covalent coupling of organophosphorus hydrolase loaded quantum dots to carbon nanotube/Au nanocomposite for enhanced detection of methyl parathion. Biosens. Bioelectron. 25 (6), 1370–1375.

Du, D., Wang, M., Zhang, J., Cai, H., Tu, H., Zhang, A., 2008. Application of multi-walled carbon nanotubes for solid-phase extraction of organophosphate pesticide. ELectrochem. Commun. 10 (1), 85–89.

Fidder, A., Hulst, A.G., Noort, D., de Ruiter, R., van der Schans, M.J., Benschop, H.P., Langenberg, J.P., 2002. Retrospective detection of exposure to organophosphorus anti-cholinesterases: mass spectrometric analysis of phosphylated human butyrylcholinesterase. Chem Res. Toxicol. 15 (4), 582–590.

Giordano, B.C., Collins, G.E., 2007. Synthetic methods applied to the detection of chemical warfare nerve agents. Curr. Org. Chem. 11 (3), 255–265.

Hariharasubramanian, A., Ravichandran, Y.D., Rajesh, R., Rajkumari, R., Selvan, G.K., Arumugam, S., 2014. Functionalization of multi-walled carbon nanotubes with 6-aminobenzothiazole and their temperature-dependent magnetic Studies. Fuller. Nanotub. Carbon Nanostruct. 22 (10), 874–886.

Hu, H., Liu, X., Jiang, F., Yao, X., Cui, X., 2010. A novel chemiluminescence assay of organophosphorous pesticide quinalphos residue in vegetable with luminol detection. Chem. Cent. J. 4, 13.

Huang, Y., Zhou, Q., Xiao, J., Xie, G., 2010. Determination of trace organophosphorus pesticides in water samples with TiO_2 nanotubes cartridge prior to GC-flame photometric detection. J. Sep. Sci. 33 (14), 2184–2190.

Iijima, S., 1991. Helical microtubules of graphitic carbon. Nature 354 (6348), 56–58.

Karami, A., Latifi, A.M., Khodi, S., 2014. Comparison of the organophosphorus hydrolase surface display using InaVN and Lpp-OmpA Systems in *Escherichia coli*. J. Microbiol. Biotech. 24 (3), 379–385.

Kumar, P., Kim, K., Deep, A., 2015. Recent advancements in sensing techniques based on functional materials for organophosphate pesticides. Biosens. Bioelectron. 70, 469–481.

Kweon, H.K., Hakansson, K., 2006. Selective zirconium dioxide-based enrichment of phosphorylated peptides for mass spectrometric analysis. Anal. Chem. 78 (6), 1743–1749.

Lei, Y., Mulchandani, A., Chen, W., 2005a. Improved degradation of organophosphorus nerve agents and p-nitrophenol by Pseudomonas putida JS444 with surface-expressed organophosphorus hydrolase. Biotechnol. Progr. 21 (3), 678–681.

Lei, Y., Mulchandani, P., Chen, W., Wang, J., Mulchandani, A., 2004a. Whole cell amperometric biosensor for organophosphorus nerve agents. Abstracts of papers of the American Chemical Society 227(1), U124.

Lei, Y., Mulchandani, P., Chen, W., Wang, J., Mulchandani, A., 2004b. Arthrobacter sp JS443-based whole cell amperometric biosensor for p-nitrophenol. Electroanalysis 16 (24), 2030–2034.

Lei, Y., Mulchandani, P., Wang, J., Chen, W., Mulchandani, A., 2005b. Highly sensitive and selective amperometric microbial biosensor for direct determination of p-nitrophenyl-substituted organophosphate nerve agents. Env. Sci. Technol. 39 (22), 8853–8857.

Li, D., Xia, Y.N., 2003. Fabrication of titania nanofibers by electrospinning. Nano Lett. 3 (4), 555–560.

Li, Z., Wang, Y., Ni, Y., Kokot, S., 2014. Unmodified silver nanoparticles for rapid analysis of the organophosphorus pesticide, dipterex, often found in different waters. Sens. Actuators B-Chem. 193, 205–211.

Liu, G., Guo, W., Yin, Z., 2014. Covalent fabrication of methyl parathion hydrolase on gold nanoparticles modified carbon substrates for designing a methyl parathion biosensor. Biosens. Bioelectron. 53, 440–446.

Mulchandani, A., Chen, W., Mulchandani, P., Wang, J., Rogers, K.R., 2001. Biosensors for direct determination of organophosphate pesticides. Biosens. Bioelectron. 16 (4–5), 225–230.

Mulchandani, A., Mulchandani, P., Chen, W., Wang, J., Chen, L., 1999. Amperometric thick film strip electrodes for monitoring organophosphate nerve agents based on immobilized organophosphorus hydrolase. Anal. Chem. 71 (11), 2246–2249.

Mulchandani, P., Chen, W., Mulchandani, A., 2001. Flow injection amperometric enzyme biosensor for direct determination of organophosphate nerve agents. Env. Sci. Technol. 35 (12), 2562–2565.

Mulchandani, P., Chen, W., Mulchandani, A., 2006. Microbial biosensor for direct determination of nitrophenyl-substituted organophosphate nerve agents using genetically engineered Moraxella sp. Anal. Chim. Acta 568 (1–2), 217–221.

Mulchandani, P., Mulchandani, A., Kaneva, I., Chen, W., 1999. Biosensor for direct determination of organophosphate nerve agents. 1. Potentiometric enzyme electrode. Biosens. Bioelectron. 14 (1), 77–85.

Nasr, M., Abou Chaaya, A., Abboud, N., Bechelany, M., Viter, R., Eid, C., Khoury, A., Miele, P., 2015. Photoluminescence: A very sensitive tool to detect the presence of anatase in rutile phase electrospun TiO_2 nanofibers. Superlattice Microstruct. 77, 18–24.

Oliveira, A.M., Silva, G.A., Poppi, R.J., Augusto, F., 2008. Isolation and quantification of dialkylmercury species by headspace solid phase microextraction and gas chromatography with atomic emission detection. J. Braz. Chem. Soc. 19 (5), 1041–1047.

Park, O., Jeevananda, T., Kim, N.H., Kim, S., Lee, J.H., 2009. Effects of surface modification on the dispersion and electrical conductivity of carbon nanotube/polyaniline composites. Scr. Mater. 60 (7), 551–554.

Pedrosa, V.A., Paliwal, S., Balasubramanian, S., Nepal, D., Davis, V., Wild, J., Ramanculov, E., Simonian, A., 2010. Enhanced stability of enzyme organophosphate hydrolase interfaced on the carbon nanotubes. Colloid Surf. B 77 (1), 69–74.

Perez-Ruiz, T., Martinez-Lozano, C., Tomas, V., Martin, J., 2005. Flow injection chemiluminescent determination of N-nitrosodimethylamine using photogenerated tris(2,2′-bipyridyl) ruthenium (III). Anal. Chim Acta 541 (1–2), 69–74.

Shimazu, M., Mulchandani, A., Chen, W., 2001. Cell surface display of organophosphorus hydrolase using ice nucleation protein. Biotechnol. Progr. 17 (1), 76–80.

Shimazu, M., Mulchandani, A., Chen, W., 2003. Thermally triggered purification and immobilization of elastin-OPH fusions. Biotechnol. Bioeng. 81 (1), 74–79.

Stoytcheva, M., Zlatev, R., Gochev, V., Velkova, Z., Montero, G., 2014. Amperometric biosensor precision improvement: application to organophosphorus pesticide determination. Anal. Methods 6 (20), 8232–8238.

Tang, X., Zhang, T., Liang, B., Han, D., Zeng, L., Zheng, C., Li, T., Wei, M., Liu, A., 2014. Sensitive electrochemical microbial biosensor for p-nitrophenylorganophosphates based on electrode modified with cell surface-displayed organophosphorus hydrolase and ordered mesopore carbons. Biosens. Bioelectron. 60, 137–142.

Walorczyk, S., 2007. Development of a multi-residue screening method for the determination of pesticides in cereals and dry animal feed using gas chromatography-triple quadrupole tandem mass spectrometry. J. Chromatogr. A 1165 (1–2), 200–212.

Wang, J., Chen, L., Mulchandani, A., Mulchandani, P., Chen, W., 1999. Remote biosensor for in-situ monitoring of organophosphate nerve agents. Electroanalysis 11 (12), 866–869.

Wang, K., Li, H., Wu, J., Ju, C., Yan, J., Liu, Q., Qiu, B., 2011. TiO_2-decorated graphene nanohybrids for fabricating an amperometric acetylcholinesterase biosensor. Analyst 136 (16), 3349–3354.

White, B.J., Harmon, H.J., 2005. Optical solid-state detection of organophosphates using organophosphorus hydrolase. Biosens. Bioelectron. 20 (10), 1977–1983.

Yan, Y.M., Zhang, M.N., Gong, K.P., Su, L., Guo, Z.X., Mao, L.Q., 2005. Adsorption of methylene blue dye onto carbon nanotubes: A route to an electrochemically functional nanostructure and its layer-by-layer assembled nanocomposite. Chem. Mater. 17 (13), 3457–3463.

Yang, Y., Tu, H., Zhang, A., Du, D., Lin, Y., 2012. Preparation and characterization of Au-ZrO_2-SiO_2 nanocomposite spheres and their application in enrichment and detection of organophosphorus agents. J. Mater. Chem. 22 (11), 4977–4981.

Zhang, J., Lee, J.K., Wu, Y., Murray, R.W., 2003. Photoluminescence and electronic interaction of anthracene derivatives adsorbed on sidewalls of single-walled carbon nanotubes. Nano Lett. 3 (3), 403–407.

Zhou, M., Guo, L., Lin, F., Liu, H., 2007. Electrochemistry and electrocatalysis of polyoxometalate-ordered mesoporous carbon modified. Anal. Chim. Acta 587 (1), 124–131.